PCCP

Elastic Moduli of Normal and Cancer Cell Membranes Revealed by Molecular Dynamics Simulations

Journal:	*Physical Chemistry Chemical Physics*
Manuscript ID	CP-ART-10-2021-004836.R2
Article Type:	Paper
Date Submitted by the Author:	12-Feb-2022
Complete List of Authors:	Nguyen, Hoang Linh; Institute for Computational Science and Technology, Man, Viet Hoang; University of Pittsburgh Li, Mai Suan; Institute of Physics , Polish Academy of Sciences Derreumaux, Philippe; University Paris Diderot - Paris 7, UPR9080 CNRS Wang, Junmei; University of Pittsburgh, Department of Pharmaceutical Sciences Nguyen, Phuong; Laboratoire de Biochimie Theorique, UPR 9080 CNRS, IBPC

Elastic Moduli of Normal and Cancer Cell Membranes Revealed by Molecular Dynamics Simulations

Hoang Linh Nguyen,[†] Viet Hoang Man,[‡] Mai Suan Li,[¶,†] Philippe Derreumaux,[§] Junmei Wang,[‡] and Phuong H. Nguyen[*,§]

†*Institute for Computational Science and Technology, SBI Building, Quang Trung Software City, Tan Chanh Hiep Ward, District 12 , Ho Chi Minh City, Vietnam*

‡*Department of Pharmaceutical Sciences, School of Pharmacy, University of Pittsburgh, Pittsburgh, PA 15213, USA*

¶*Institute of Physics, Polish Academy of Sciences, Al. Lotnikow 32/46, 02-668 Warsaw, Poland*

§*CNRS, Université de Paris, UPR9080, Laboratoire de Biochimie Théorique, Paris, France ; Institut de Biologie Physico-Chimique, Fondation Edmond de Rothschild, PSL Research University, Paris, France*

E-mail: nguyen@ibpc.fr

Abstract

Recent studies indicate that there are mechanical differences between normal cells and cancer cells. Because the cell membrane takes part in a variety of vital processes, we test the hypothesis whether two fundamental alterations in the cell membrane: the overexpression of phosphatidylserine lipids in the outer leaflet and the reduction of cholesterol concentration could cause the softening in cancer cells. Adopting ten models of the normal and cancer cell membranes, we carry out 1-μs all-atom molecular

dynamics simulations to compare the structural property and elasticity property of two membrane types. We find that the overexpression of the phosphatidylserine lipids in the outer leaflet does not significantly alter the area per lipid, the membrane thickness, the lipid order parameters and the elasticity moduli of the cancer membranes. However, a reduction in the cholesterol concentration leads to clearly changes in those quantities, especially decreases in the bending, tilt and twist moduli. This implies that the reduction of cholesterol in the cancer membranes could contribute to the softening of cancer cells.

Introduction

Cancer is a serious problem affecting the health of all human societies. Basically, it is the uncontrolled growth of abnormal cells in the body. These cells have the ability to spread, leading to the appearance of tumors in organs located far away from the primary tumor site.[1] During the spread, cancer cells must pass through many obstacles such as small gaps of basement membrane, blood vessel and crowded environments in the body. Therefore, it has been suggested that cancer cells must be soft and deformable to perform such task.[2] Indeed, a growing number of experimental techniques are being used to study the mechanical properties of cancer cell lines or primary cells from biopsies,[3–5] and results clearly indicate that cancer cells from a large number of different organs are softer than their normal counterparts. This may be due to alterations in the extracellular environment, as well as in the intracellular elements such as cell microenvironment, the cytoskeleton, the nucleus, the intracellular compartments, the signalling proteins, the active forces, the internal membrane and the plasma membrane.[2] Understanding which cell elements contribute to the softness of cancer cells could be very important for the development of efficient diagnosis and treatment methods. In this work, we only focus on the cell membrane element, and try to understand whether fundamental alterations in the membrane properties cause the cancer cells to be softer than the normal counterparts.

Normal cell membranes have a highly asymmetric lipid composition.[6] That is, the extracellular leaflet is mainly composed of phosphatitylcholine (PC) and sphingo lipids, and the intracellular leaflet is mostly composed of phosphatudylethanolamine (PE) and phosphatidylserine (PS) lipids. Is is known that the concentration of the negatively charged PS lipids is increased by 5-9 times in the outer leaflet when normal membranes are transformed to cancer membranes, and this is usually considered as a biological cue related to the apoptotic pathway.[7,8] As a consequence, the cancer membranes have less negative membrane potential than that of the normal membranes.[9–11] Another alteration in cancer cells is the reduction of cholesterol in their membranes,[12] which results in decreases of the order of lipid hydrocarbon chains and membrane thickness, and increase of surface area of lipids.[13–17] However, effects due to the reduction of cholesterol and overexpression of negatively charged PS lipids in the outer leaflet on the elastic property of cancer membranes have so far not been studied to the best of our knowledge.

Molecular dynamics (MD) simulations have provided valuable informations on structural and dynamical properties of lipid bilayers. In the early days, MD simulations of membrane models considered only a single-component lipid bilayers,[18–20] later simulations have incorporated more than one lipid component as well as cholesterol.[21] However, many of these multiple-component lipids simulations were performed on symmetric bilayers containing the same lipid mole fractions of both leaflets. Recently, several MD simulations on asymmetric bilayers have also been reported.[6,22,23] Despite many MD simulations of lipid membranes have been carried out, there is little work on the modelling of the membrane of cancer cells. Only several cancer membrane computational models have been recently developed.[24–26]

The main aim of this work is to employ MD simulation to theoretically study effects of the two mentioned alterations, i.e, the overexpression of the PS lipid concentration in the extracellular leaflet, and the reduction of the cholesterol concentration on the elasticity property of normal and cancer membranes. This may provide some insights into the differences in the mechanical properties of two cell types. From the theoretical side, many studies have

used the traditional Canham-Helfrich model of membrane fluctuations to calculate the bending modulus K_c.[27,28] Latter, May et al. have extended this model to include the molecular tilting.[29] This extension is widely considered to be important for understanding membrane fusion.[30] Recently, Watson et al. have provided a theoretical model to include three moduli elastic moduli, i.e, bending, tilt and twist, which can be extracted from MD simulation data in the Fourier space.[31–34] Very recently, Khelashvili et al. have developed a method which allows for calculating the bending K_c modulus from local fluctuations on the molecular scale in the real space.[35–38] From the experimental side, for many years, experiments have used the Canham-Helfrich model to analyse diffuse X-ray scattering in order to obtain values for K_c.[39] Unfortunately, results of K_c of chemical identical membranes, obtained from different experiments, are usually substantially different,[40] even for single component lipid membranes. Furthermore, there are nearly no experimental data for multiple components lipid membranes.

In this work, we carry out all-atom MD simulations of five normal membrane models and five cancer membrane models taken from previous works.[24–26] All these models have the same lipid compositions, the same number of total lipids, but differ in the lipid mole fractions of the outer and inner leaflets, and in the cholesterol concentration. From simulation data, various structural quantities are characterized, and the bilayer bending, tilt and twist moduli are calculated, allowing us to compare the structure and elasticity property of the normal and cancer membranes.

Methodology

Membrane models

First, we construct four normal membrane models based on the models of previous works. Rivel et al.[24] constructed models using the lipid contents of the mammalian erythrocyte membrane obtained by two different experiments.[41,42] Based on their models, and using the

same mole fractions of lipids and cholesterol, we construct two normal membrane models named as M1 and M2. Our third normal membrane model, named M3, is constructed using the lipid mole fractions of the model of Klahn et al.,[25] which was built using another experimental data of erythrocyte cells.[43] The fourth normal membrane model (M4) is built using the mole fractions of lipids of the model of Ingolfsson et al., which was constructed using the general properties of cell membranes found within the brain.[26] Each model contains four lipid types: 1,2-dioleoyl-sn-glycero-3-phosphocholine (DOPC), sphingomyelin lipids (SM), dioleoyl-sn-glycero-3-phosphoethanolamine (DOPE) and 1,2-dioleoyl-sn-glycero-3-phospho-L-serine (DOPS) lipids. Following the work of Rivel et al., we add $\sim 33\%$ cholesterol (CHL) to each membrane model. This concentration is about the typical sterol concentration in the mammalian plasma membrane.[44] We also construct a model (M5) containing only 15% cholestrol, but the numbers of lipids are the same as that of the M1 model. These two models M1 and M5 allow us to study the effect of cholesterol reduction. The numbers of lipids and cholesterol of five normal membrane models are listed in Tab.1. As seen, the asymmetry of lipid distributions between two leaflets, which is a general feature of normal membranes, is taken into account in the construction.

Table 1: The total number of each lipid component in the outer and inner leaflets of five normal cell membrane models. The models M1 and M2 is referred to the work by Rivel et al.,[24] the model M3 is referred to the work by Klahn et al.,[25] and the M4 is referred to the work by Ingolfsson et al.[26] Model M5 is as same as model M1 but contains only half of cholesterol.

Lipid	M1		M2		M3		M4		M5	
	outer	inner	outer	inner	outer	inner	outer	inner	outer	inner
SM	84	24	76	12	90	6	56	28	84	24
DOPC	92	28	70	18	78	30	104	48	92	28
DOPE	28	92	38	110	28	100	18	70	28	92
DOPS	0	60	16	60	8	64	0	30	0	60
CHL	102	102	102	102	102	102	102	102	51	51

Having designed the normal membranes, the cancer counterparts are obtained by symmetrizing the number of lipids between two leaflets. This mimics the overexpression in

Table 2: The total number of each lipid component in the outer and inner leaflets of five cancer cell membrane models. A cancer model Mi* (i=1...5) is obtained by symmetrising the number of lipids between the outer and inner leaflets of the normal membrane model Mi counterpart shown in Tab.1.

Lipid	M1*		M2*		M3*		M4*		M5*	
	outer	inner	outer	inner	outer	inner	outer	inner	outer	inner
SM	54	54	44	44	48	48	42	42	54	54
DOPC	60	60	44	44	54	54	76	76	60	60
DOPE	60	60	74	74	38	64	44	44	60	60
DOPS	30	30	38	38	16	36	16	16	30	30
CHL	102	102	102	102	102	102	102	102	51	51

PS/PE in the outer leaflets of cancer membranes. The population of cholesterol is kept the same between two leaflets. The number of lipids of five cancer membrane models is listed in Tab.2.

Simulation method

Given the number of lipids listed in Tabs.1 and 2, we use the CHARMM-GUI serve to build the membranes. The all-atom CHARMM36 force field[45] and the TIP3P water model[46] are used to model the lipids and solvent, respectively. The initial dimensions of the unit cell are $(L_x, L_y, L_z) = (12, 12, 9)$ nm. Starting from each initial structure, an equilibrium MD simulation is carried out for 100 ns, followed by a production run for 1000 ns in the NPT ensemble with the pressure $P_0 = 1$ bar and temperature $T = 300$ K. The GROMACS simulation package[47] is used for the simulation. The Berendsen coupling methods[48] are used to maintain the pressure and temperature of the system at the desired values with the coupling constants of 0.1 ps. The equations of motion are integrated using the leapfrog algorithm with a small time step of 2 fs. The electrostatic interactions are calculated using the particle mesh Ewald method and a cutoff of 1.4 nm.[49] A cutoff of 1.4 nm is used for the van der Waals interactions. The nonbonded pair lists are updated every 5 fs. The data is saved for every 10 ps for subsequent analyses.

Membrane elastic moduli

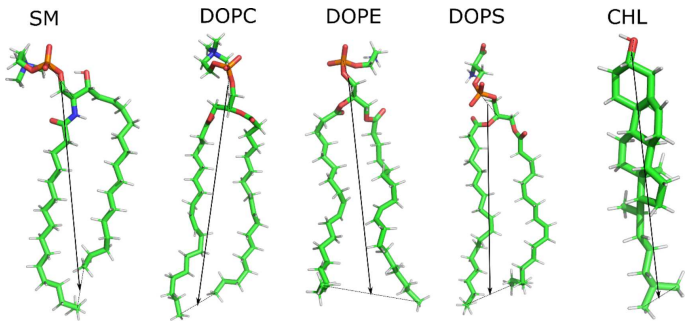

Figure 1: The molecular structure of lipids and cholesterol used to construct the membranes in this work. The orientation of a lipid is described by a black unit vector. See text for detailed definition.

From the simulation data, we calculate the elastic moduli of membranes employing the method recently developed by Levine et al.[31–33] It is useful to briefly describe the method here, and the readers are referred to Refs.[31–33] for more details. First, the orientation of a lipid is characterised by a unit vector $\mathbf{n}^\alpha$ which points from the midpoint between phosphorus and glycerol C2 atoms of the head group to the midpoint between the two terminal methyl carbons of two lipid tails. For the cholesterol, the unit vector joins C3 and C17 atoms [Fig.1]. Here, $\alpha = 1$ and 2 denote the lipids belonging to the outer and inner leaflets, respectively. Let $\mathbf{u}_r^\alpha(\mathbf{r})$, $(\mathbf{r} = \mathbf{r}(x, y))$ be the projection vector of the vector $\mathbf{n}^\alpha$ on the xy plane of the membrane, and $\mathbf{u}_q^\alpha(\mathbf{q})$ be the Fourier transformed of $\mathbf{u}_r^\alpha(\mathbf{r})$ .The orientation vector of the bilayer is then defined as $\mathbf{u}_q(\mathbf{q}) = [\mathbf{u_q^1}(\mathbf{q}) - \mathbf{u_q^2}(\mathbf{q})]/\mathbf{2}$. This vector is then decomposed into longtitudinal component $\mathbf{u}_q^{\parallel} = 1/q[\mathbf{q}.\mathbf{u}_q]$ and transverse component $\mathbf{u}_q^{\perp} = 1/q[\mathbf{q} \times \mathbf{u}_q)].\hat{z}$. It has been shown that[31–33]

$$\langle |\mathbf{u}_q^{\parallel}|^2 \rangle = \frac{k_{\mathrm{B}}T}{K_c q^2}, \quad \langle |\mathbf{u}_q^{\perp}|^2 \rangle = \frac{k_{\mathrm{B}}T}{K_\theta + K_{\mathrm{tw}} q^2} \tag{1}$$

where T is temperature, k_{B} is Boltzmann's constant, K_c, K_θ and K_{tw} are the bilayer bending, lipid tilt and twist moduli, respectively.

We also calculate the bending modulus K_c using the local real-space method of Khe-

lashvili et al.[35] First, a potential of mean force of the angle α between two neighbouring lipid unit vectors $\mathbf{n}^{\alpha}$ is extracted from the simulation

$$U(\alpha) = -k_B T \ln[\frac{P(\alpha)}{\sin(\alpha)}], \tag{2}$$

where $P(\alpha)$ is the probability distribution of α over all configurations, and all lipid pairs. A lipid pair is considered if two lipids are separated by less than 1 nm, and at least one unit vector is oriented less than or equal to 10 degrees from the bilayer normal. The splay modulus χ^{ij} between a pair of lipids is obtained by fitting the plot of Eq.4 to a functional form

$$U(\alpha) = \frac{1}{2}\chi^{ij}\alpha^2 + c, \tag{3}$$

where c is a constant, and the fit is limited to small values of α in a range of 10-30 degrees. The bending modulus K_c is then calculated as

$$\frac{1}{K_c} = \frac{1}{\phi_{\text{total}}} \sum_{\langle i,j \rangle} \frac{\phi_{i,j}}{\chi^{ij}}, \tag{4}$$

where ϕ_{ij} is the number of i, j neighbouring pair, and ϕ_{total} is the total number of ϕ_{ij} for all pairs.

Results

Structural properties

Lipid surface area

To obtain the first impression on the structural property of the membranes, we calculate the average area occupied by individual lipids (area per lipid, A_L) pertaining to the outer and inner leaflets of each membrane model. We employ the method recently developed by Gapsys et al.,[50] which is based on the GridMAT-MD algorithm[51] and implemented to GROMACS

Table 3: The area per lipid (A_L) and the thickness (d) of the normal (M1$\cdots$ M5) and cancer (M1*$\cdots$ M5*) membranes. The area per lipid is shown for the outer and inner leaflets. Shown are results averaged over 1 microsecond trajectories at 300 K.

Membrane model	A_L [Å^2]		d [Å]
	outer	inner	
M1	54.24±0.13	54 .30±0.17	42.6±0.3
M1*	54.28±0.14	53.95±0.14	42.7±0.3
M2	53.90±0.16	53.82±0.12	42.6±0.3
M2*	54.20±0.13	54.46±0.13	42.4±0.2
M3	53.68 ±0.14	54.19±0.13	42.7±0.4
M3*	54.34±0.13	54.13±0.12	42.5±0.3
M4	51.74±0.15	51.94±0.11	42.3±0.4
M4*	52.48±0.11	52.27±0.14	42.2±0.2
M5	56.27±0.19	56.39±0.18	41.6±0.2
M5*	55.99 ±0.18	56.24 ±0.16	41.8 ±0.2

as the analysis tool $g_{lomepro}$. The time evolution and histogram distribution of A_L of all membrane models are shown in Figs. S1 and S2. The results show that the structure of membranes has relaxed to a reasonable state and is stable during the simulation timescale of 1 microsecond. The time average of A_L listed in Tab.3 indicate that although there are differences in the mole fraction of lipids between normal membranes, between cancer membranes, between two leaflets, or between normal and cancer membranes, the areas per lipid of all models are quite similar, lying in the range $\sim 51.74 - 54.46$ Å^2. This is a typical range of A_L of common lipid bilayers previously reported by experiments and atomistic simulations.[52] The area per lipid values of models M4 and M4* are rather lower than the other models. This is because M4 and M4* have low DOPS and DOPE concentrations [Tabs.1, 2], and moreover the size of the serine group of DOPS, and of the ethanolamine group of DOPE is smaller than the choline group of other lipids. At a lower cholesterol concentration of 15%, the areas per lipid of models M5 and M5* are higher than that of the M1 and M1* counterparts. This is because the presence of cholesterol in lipid bilayer increases the free spaces between lipid chains,[53] thus effectively decreasing the lipid area in M1 and M1*. This effect of cholesterol was also observed by MD simulations of Klahn et

all.[25] and Shahane et al.[52] with their cancer membrane models. Overall, our results show that the area per lipid does not depend much on the used models, is not affected much by the overexpression of the DOPS lipid in the outer leaflet, but is increased as the cholesterol concentration decreases.

Electron density and membrane thickness

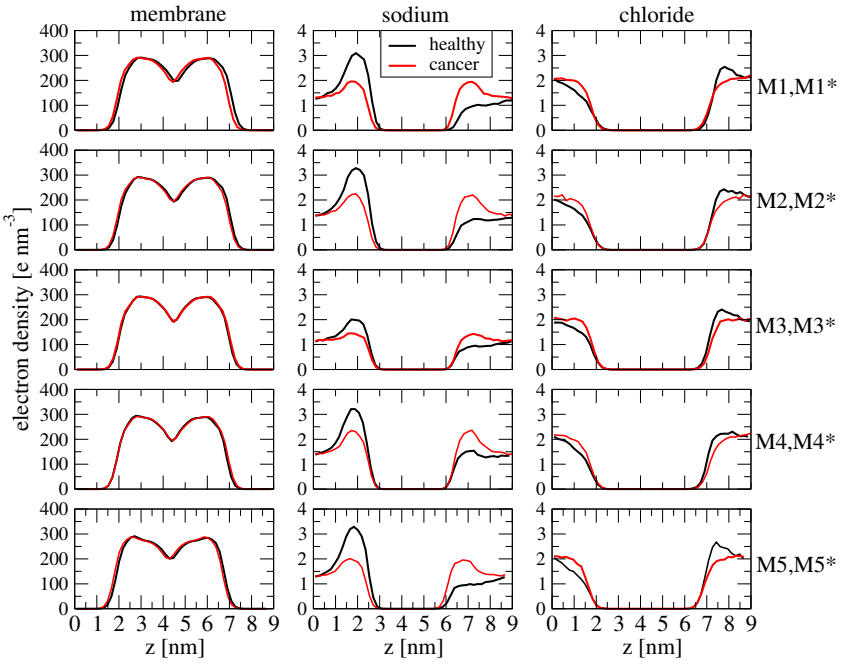

Figure 2: The electron density profile of the lipid membrane (left panels), the sodium ions (middle panels) and chloride ions (right panels) along the z-direction. Shown are results of the normal (black) and cancer (red) membranes.

To understand effects induced by the overexpression of the negatively charged DOPS lipids in the outer leaflet of the cancer membranes, we calculate the electron density of the normal and cancer membrane models along the z-dierection, and results are shown in Fig.2. As seen, the density profiles of the membrane of the models M1$\cdots$ M4 and M1*$\cdots$ M4*, which have the same cholesterol concentration of 33%, are not significantly different. Thus, the membrane thickness, which is measured as the distance between two maxima of the average electron density in z-direction, of all models are also quite similar, $\sim$ 4.2 nm [Tab.3],

which agree with previous results of experiment,[17] and simulations.[25,52] The reduction of cholesterol in the models M5 and M5* results in a slightly decrease ($\lesssim 10\%$) in the thickness. This is because an increase in cholesterol causes a decrease in the lipid surface area, and because a lipid membrane behaves as an incompressible fluid, thus the bilayer thickness is increased. In all cases, the time evolution of the thickness of all membranes undergoes some fluctuations within the first 400 ns before relaxing to a stable value, indicating the convergence of the simulations [Figs. S3, S4]. We also calculate the electron density of the sodium cations and chloride anions in the direction perpendicular to the membrane of all models and the profiles are also shown in Fig.2. Due to the asymmetry in the distribution of lipids in normal membranes, the interactions of the outer and inner leaflets with ions are different, resulting an asymmetry in the profiles, with a low and and high densities of sodium on the outer ($z \geq 5$ nm) and inner ($z \leq 5$ nm) leaflets, respectively. In contrast, the densities of chloride are high and low on the outer and inner leaflet, respectively. The increase of the negatively charged DOPS lipids in the outer leaflet of the cancer membranes results in the increase and decrease of the sodium and chloride concentration on the surface of that leaflet, respectively. This was also observed by the simulation of Klahn et al.[25] whose membrane models are similar to our M3, M3* models. Due to the difference in the lipid mole fractions between normal membrane models, or between cancer membrane models, there are slightly differences in the peaks of the density profiles of ions. For example, the peak of the sodium profile is about 3 e/nm^3 for M1 but only 2 e/nm^3 for M3 at $z \geq 1.5$ nm. A comparison of the model M1 (M1*) with the counterpart M5 (M5*) shows that change in the cholesterol concentration does not lead to significant changes in the electron density of the membranes as well as of the ions. Overall, our simulations show that the electron density profile of lipid bilayers are similar for all membrane models regardless theirs difference in the lipid and cholesterol concentrations, but the electron densities of ions on the membrane surfaces slightly depend on the membrane models and differ between normal and cancer membranes.

Lipid order parameters

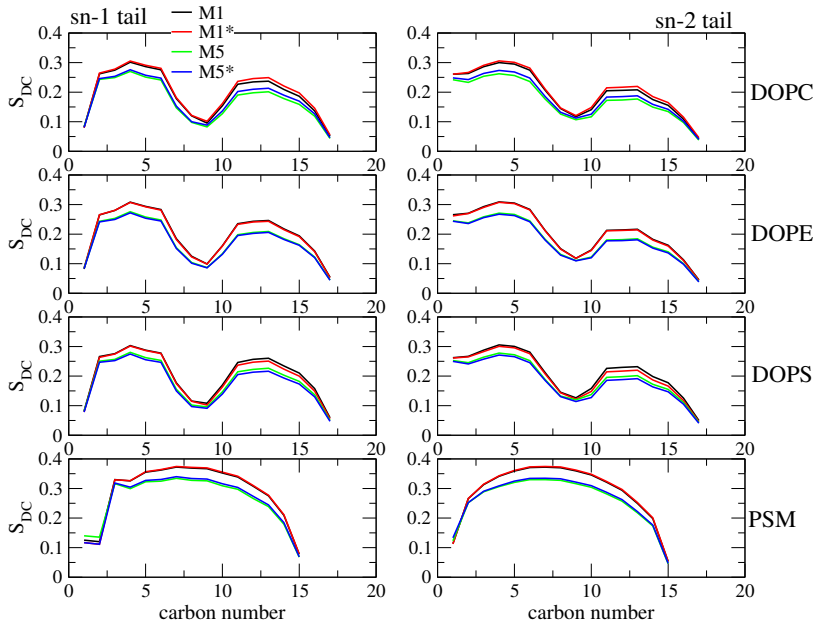

Figure 3: Comparison of the order parameters for the two tails sn-1 (left) and sn-2 (right) of four lipid types DOPC, DOPE, DOPS and SM of the normal (M1, M5) and cancer (M1*, M5*) membrane models. Carbon atom numbers increase in the direction of the tail termini. Shown are results averaged over 1000 ns trajectories at 300 K.

Next, we wish to understand whether the ordering of lipid acyl chain tails depends on the membrane models, and exhibits any difference between the normal and cancer membranes. Here, an order parameter is defined as $S_{\mathrm{CH}} = \langle 3\cos^2\theta - 1\rangle/2$, where θ is the angle between a C-H bond vector and the bilayer normal.[54] The angular brackets represent molecular and temporal ensemble averages. Values of S_{CH} vary between 1 where all CH_2 groups are forming a straight line, and 0 if all possible angles θ are found with the same probability. For the DOPC, DOPE and DOPS lipids, each tail consists of 17 order parameters, and for SM lipids, each tail consists of 15 order parameters. We find that the order parameters of lipids in all models are very similar, and Fig.3 shows, as examples, the results of the M1, M1* models and theirs less cholesterol counterparts M5, M5*. As seen, the values are superposable between the normal and cancer models M1, M1* or M5, M5*, and also similar to those reported in

literature.[54] It is known that the presence of cholesterol in lipid membranes increases the ordering of lipid chains,[53] and this is also seen from our simulation, showing that the lipid order parameters of M5 or M5* are lower than that of M1 or M1* models. Overall, the results indicate that the lipid orientational order does not sensitively depend on the difference in the lipid mole fractions of models, regardless normal or cancer types, and on the overexpression of the DOPS lipids in the outer leaflet, but does decrease with the decrease of the cholesterol concentration.

Membrane electrostatic potential

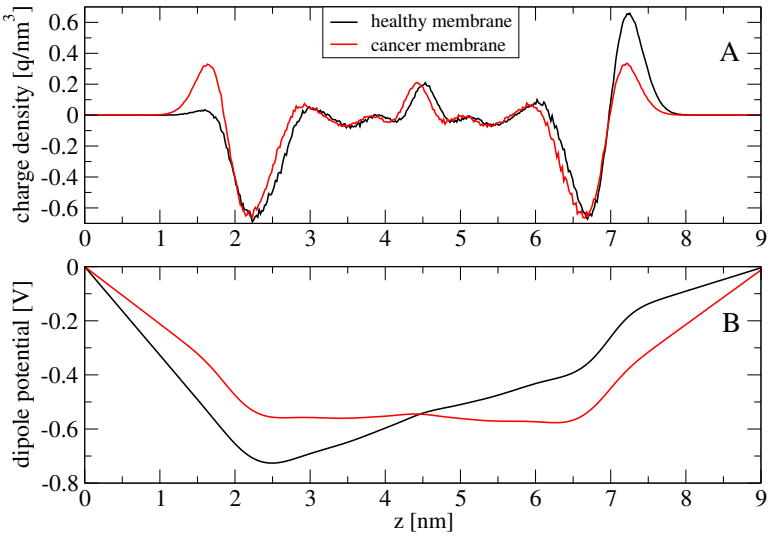

Figure 4: The charge density (A) and the dipole potential (B) profiles along the z-direction. Shown are results of the normal (black) and cancer (red) membrane models M1 and M1*.

The electrostatic potential across the membrane $\Psi(z)$ is related to the charge density $\rho(z)$ along the membrane normal z via the Poisson equation

$$\frac{d^2\Psi(z)}{dz^2} = -\frac{\rho(z)}{\epsilon_0}. \tag{5}$$

where ϵ_0 is the electrostatic permittivity of vacuum. Because the simulations have been done with periodic boundary condition, thus we impose condition $\Psi(0) = \Psi(L)$ where L is the simulation box length in z-direction. By choosing $z = 0$ at the corner of the simulation box and set $\Psi(0) = 0$, the potential can be calculated as[55]

$$\Psi(z) = -\frac{1}{\epsilon_0}\int_0^z (z-t)\rho(t)dt + \frac{z}{\epsilon_0 L}\int_0^L (L-t)\rho(t)dt. \quad (6)$$

In practice, the charge density $\rho(z)$ is calculated by dividing the whole box into 500 slabs of 0.018Å parallel to the x-y plane and counting the number of charges in each slab. As an example, Fig.4(A) shows the charge density profile of the normal and cancer membranes M1 and M1*. The dominant positive peak in the outer leaflet at $z \sim 7 - 7.5$ nm of M1 is mainly contributed by the positively charged choline groups of highly populated DOPC and SM lipids. The negative peaks at $z \sim 6.5 - 7$ nm (outer leaflet) and $z \sim 2 - 2.5$ nm (inner leaflet) are similar, and both come from the negatively charged phosphate groups of DOPC, DOPE and SM lipids. Due to high population of DOPS lipids in the inner leaflet of the normal membranes, their negatively charged serine groups compensate with the positively charged groups of DOPC, DOPE, SM, leading a low peak in the profile at $z \sim 1 - 1.5$ nm. As expected, the charge profile of cancer membrane M1* is symmetric due to the symmetry of two leaflets. For both membranes, the peaks at the membrane center are quite high, and come mainly from the partial charges on the terminal methyl group at the lipid tails. Fig.4(B) shows the potential obtained from Eq.6 with density from Fig.4(A). Due to high negatively density in the inner leaflet of M1, the electrostatic potential in this leaflet is more negative than that in the outer leaflet. Again, the potential profile of M1* is symmetric between two leaflets, with peaks in are higher and lower than that of M1 in the inner and outer leaflets, respectively. The charge density and electrostaic potential profiles of the other normal or cancer models show the similar behaviour as those of M1 or M1*. Overall, our simulation shows that the electrostatic potential of the normal membrane is asymmetric,

with a downhill slope on going from the outer leaflet to the inner leaflet. In contrast, the electrostatic profile of the cancer membrane is symmetric and rather flat. This indicates that the electrostatic potential is indeed affected by the overexpression of the DOPS lipid in the outer leaflet of the cancer membranes.

Membrane elastic property

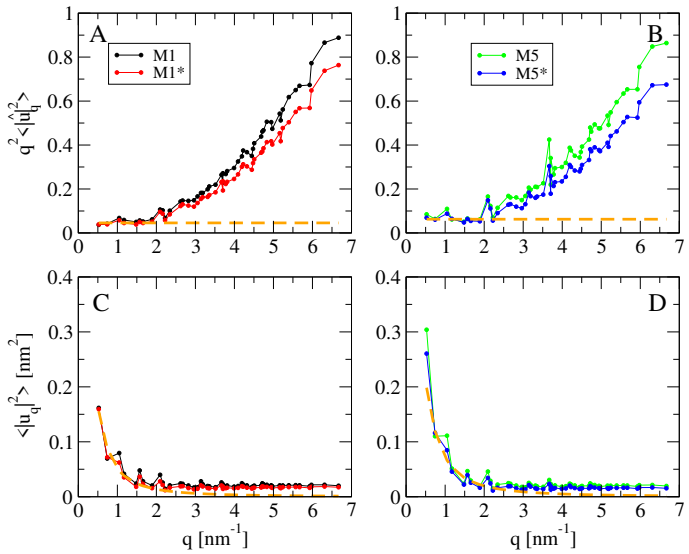

Figure 5: Power spectra of the longitudinal (weighted by q^2) (A, B) and transverse (C, D) components of the lipid orientation vector. Shown are results of the high cholesterol membrane models M1, M1* (A, C) and low cholesterol membrane models M5 and M5* (B, D). The best fits of the data to Eq.1 are shown by the orange dotted lines. Only data points in the range $0 < q < 1.5$ nm^{-1} are used for the fit of the longitudinal curves, and $0 < q < 3.5$ nm^{-1} for the transverse curves. The spectra are averaged over 1000 ns trajectories.

Having compared the normal and cancer membranes in terms of structural properties, in the following we compare their elastic properties. From simulation data, we extract the orientation vectors $\mathbf{u}_\mathbf{r}^\alpha$ of the lipid and cholesterol molecules, and the power spectra as a function of the wavelength q are calculated from Eq.1. The spectra are averaged over 1000 ns, and shown in Fig.5, as an example, for the M1 and M1* models. As seen, the spectra $\langle|\mathbf{u}_q^{\parallel}|^2\rangle$ (weighted by q^2) is almost constant with $q < 1.5$ nm^{-1} or equivalently $r > 2\pi/q \approx 4.2$ nm [Figs.5(A,B)]. In this plateau region the theoretical prediction for K_c, Eq.1, is valid, and this

Table 4: The bending (K_c), tilt (K_θ) and twist ($K_{\rm tw}$) elastic moduli of the normal (M1$\cdots$ M5) and cancer (M1*$\cdots$ M5*) membrane models calculated using Eq.1. The bending modulus $K_c^{'}$ is calculated using Eq.4. Shown are results at temperature of 300 K obtained using the analysis of the fluctuation of the lipid orientation vector method. The error bars are obtained using the block average method with 5 data blocks, each 200 ns long.

Models	$K_c(10^{-20}$ J)	$K_\theta(10^{-20}$ J/nm^2)	$K_{\rm tw}(10^{-20}$ J)	$K_c^{'}(10^{-20}$ J)
M1	10.5 ± 0.7	4.2 ± 0.5	1.3 ± 0.1	10.33 ± 0.8
M1*	10.6 ± 0.8	4.0 ± 0.6	1.6 ± 0.1	10.29 ± 0.8
M2	11.5 ± 0.3	4.3 ± 0.3	1.5 ± 0.1	10.32 ± 0.9
M2*	11.9 ± 0.4	4.6 ± 0.7	1.6 ± 0.1	10.25 ± 0.9
M3	9.5 ± 0.6	3.9 ± 0.3	1.2 ± 0.1	10.32 ± 0.6
M3*	9.7 ± 0.7	4.4 ± 0.4	1.9 ± 0.1	10.31 ± 1.2
M4	10.2 ± 0.8	4.2 ± 0.3	1.6 ± 0.1	10.21 ± 0.9
M4*	10.6 ± 0.5	4.1 ± 0.4	1.4 ± 0.1	10.24 ± 0.8
M5	8.2 ± 0.5	1.3 ± 0.2	0.8 ± 0.1	9.87 ± 0.5
M5*	8.1 ± 0.4	1.2 ± 0.2	0.9 ± 0.1	9.84 ± 1.0

allows us to extract the constant K_c by fitting the data points to a straight line [Figs.5(A,B)]. Note that the plateau region extends over the distances $r > 4.2$ nm, which is much smaller than the length of the simulation box of 12 nm, thus results of K_c are well-converged with system size. This is an advantage of the fluctuation method, which does not require large system size as mentioned by Levine et al.[33] To obtain the tilt, K_θ, and twist, $K_{\rm tw}$, moduli, we fit the power spectra shown in Figs.5(C,D) to the theoretical prediction curve, Eq.1. Here, only data points with $0 < q < 3.5$ nm^{-1} are used for the fit. The elastic moduli of all normal and cancer membranes at 300 K are listed in Tab.4. The error bars are estimated by using five data blocks, each 200 ns.

We first compare the elastic moduli between the normal membrane models, or between the cancer models at the cholesterol concentration of 33%. To this end, we calculate the variation in each elastic modulus between any two normal membranes, or between any two cancer membranes. We find that within the error bar, the values of the bending modulus K_c of all normal membranes or all cancer membranes are basically the same. For the tilt and twist moduli, the largest variation is 10% for K_θ between M2-M3, and 25% for $K_{\rm tw}$ of pair M3-M4. The maximum differences between the cancer membrane models are 15% for K_θ of

pair M1*-M2*, and 26% for $K_{\rm tw}$ of pair M3*-M4*. These differences are more or less in the same order of the largest error bars, which are 12% for K_θ of M1, 7% for $K_{\rm tw}$ of M1, 15% for K_θ of M1*, and 7% for $K_{\rm tw}$ of M4*, indicating that the tilt and twist elastic moduli are also similar between models, regardless of the normal or cancer membrane types.

A comparison of the normal membranes with cancer membranes reveals that within the error bar, there are basically no differences in the bending, K_c, and tilt, K_θ, moduli of any transformations $\mathrm{M}_i \rightarrow \mathrm{M}^*_i$. However, there is a small difference in $K_{\rm tw}$, that is M1*, M2* and M3* are about 23%, 7% and 58% stiffer than M1, M2, and M3, respectively, but M4* is 12% softer than M4 . At a lower cholesterol concentration of 15%, the models M5 and M5* have similar bending and tilt moduli, but the twist mode of M5* is about 25% stiffer than that of M5.

A comparison between the membranes with different cholesterol concentration shows that all elastic moduli of the membranes with low cholesterol are smaller than that of membranes with high cholesterol. The normal membrane model M5 is $\sim$ 22%, 69% and 38% softer than M1 in the bending, tilt and twist modes, respectively. The cancer membrane model M5* is $\sim$ 24%, 70% and 43% softer than M1* in the bending, tilt and twist modes, respectively. All above results show that if we consider the cancer model M5* as a transformation of the normal model M1, then it is clear that the softening in the elastic moduli of M5* is mainly caused by the reduction in the cholesterol concentration, but not by the overexpression of the DOPS lipid in the outer leaflet.

We also calculate the bending modulus K_c of all membrane models using the real space method of Khelashvili et al.,[35] and results shown in Tab.4 indicate that, for each membrane model, there is essentially no difference in the bending modulus obtained by the two methods. The differences are less than 10%, except that the largest difference is about 17% for M5 or M5* models. This confirms that our results are not strongly biased due to the employed calculation methods. We note that while the method by Levine et al.[33] shows clearly effect of cholesterol concentration, the results obtained by the method of Khelashvili et al.[35] are

not clearly evident. Nevertheless, both methods do show a trend that K_c is smaller at a lower cholesterol concentration.

Overall, the results show that with the same cholesterol concentration but difference in the lipid mole fractions, the bending and tilt moduli of the different membranes, regardless of normal or cancer types, are very similar. However, there are small differences in the twist modulus between normal membrane models, between cancer membrane models, or between normal and cancer membranes. The reduction in cholesterol concentration clearly yields to low elastic moduli, i.e, softening in the membranes. This is because changes in cholesterol concentration can affect both phase behaviour[16] and phase separation[56] in lipid membranes, thereby altering, respectively, both globally[57,58] and locally[57,59] mechanical properties of membranes.

Discussion

It has been suggested that cancer cells are generally softer than normal counterparts. Several extracellular and intracellular factors could contribute to that mechanical difference.[2] In this work, we employ the atomistic MD simulation to examine whether there are any differences in the structure and elastic property of the normal and cancer cell membranes.

While the MD simulation methods of lipid membranes are well-established, it is clear that the simulation results could depend on the computational membrane models. Although biological membranes are very complex entities containing many distinct lipid species, but to be computationally feasible, most of computational models include only representative lipids. Both normal and cancer membranes of this work contain four types of lipid DOPC, DOPE, DOPS, SM and cholesterol. The cancer membranes are constructed from the normal membranes based on two fundamental transformations that are usually observed in the cancer cell membranes: the overexpression of the PS lipid population in the outer leaflet, and the reduction of the cholesterol concentration. It is clear that these models have two main limitations: they cannot represent the cell membrane of various types of cancer cells,

and other transformations are not included. For example, an increase of microvilli, which leads to large cell surfaces and the total amount of lipids,[60,61] is not considered in the models. In addition, the symmetrization of the lipid populations between the outer and inner leaflets of our cancer membrane models is oversimplified, because in reality the cancer membranes are likely to remain somewhat asymmetric. Therefore, to obtain statistically reliable results, we consider several membrane models in this work, and their results are discussed in the following.

In a previous work, Rivel et al. used different membrane models to compare the permeability of the anti-cancer drug cisplatin through the normal and cancer membranes by MD simulations.[24] Our normal models M1, M2 and cancer models M1*, M2* are constructed using the same lipid mole fractions as the models of Rivel et al. However, our models are larger to avoid the finite-size effect in the calculation of the elastic moduli. We note that Rivel et al.[24] employed the umbrella enhanced sampling technique with the total sampling of 0.5 μs to guarantee the sampling convergence of simulations, while our MD simulation is longer, 1 μs. Nevertheless, both simulations show that, given the same cholesterol concentration, various structural quantities such as the area per lipid, membrane thickness [Tab.3], the density profile [Fig.2], and the lipid order parameters [Fig.4] of the normal and cancer membranes are almost identical. This implies that the finite-size effect is negligible, and the conformational sampling of our simulation is reasonable.

Our normal model M3 is constructed using the same mole fractions of lipids of the model of Klahn et al.,[25] but again the size of our model is larger. The cancer membrane model of Klahn et al.[25] takes into account two main changes, i.e, an increase of PS lipids in the outer leaflet and a decrease of cholesterol, but the mole fractions of the other lipids in two leaflets are very similar, i.e, the cancer membrane remains somewhat asymmetry. In contrast, our cancer membrane model M3* is symmetric with the same lipid populations in two leaflet[Tab.2]. Despite the differences, their simulations and our results of M3, M3* show that the structural properties [Figs.2 and 4] of the normal and cancer models are

almost identical. This suggests that the simple symmetrization of the lipid distributions in the construction of our cancer membrane models does not affect the results.

Our normal model M4 is constructed using the same mole fractions of lipids of the realistically mammalian cell membrane models developed by Ingolfsson et al.[26] The cancer counterpart M4* is obtained by symmetrization of the distribution of lipids between the two leaflets of M4 [Tab.2]. The models of Ingolfsson et al. are very complex, consisting of different lipid species, combining different types of head groups and different types of tails asymmetrically distributed across the two leaflets. However, their MD simulations using the coarse-grained MARTINI force field show striking similarities in the overall bilayer properties such as bilayer thickness, lipid tail order, diffusion, flip-flop, and average neighbours despite significantly difference in lipid compositions between two models. Our all-atom simulations show that the structural properties of the M4 and M4* are quite similar. These results may suggest that the use of coarse-grained MARTINI or all-atom CHARMM36 force field should not yield to significant differences in the overall bilayer structural properties.

As mentioned above, Rivel et al. used the membrane models, which are similar to our M1 and M1* models, to compare the permeability of the cisplatin drug through the normal and cancer membranes.[24] Although the structural properties are similar, the authors observed that the loss of lipid asymmetry in the cancer membranes leads to decrease their permeability to cisplatin by one order of magnitude in comparison to the asymmetric membranes of normal cells. To explain this observation, the authors calculated the diffusion constant, and showed that the diffusion of cisplatin is slower in the cancer membrane than in the normal counterpart, although the energy barrier of permeation remains the same in both membranes.[24] Our simulation shows that due to the asymmetric distribution of charged lipids between the inner and outer leaflets, the electrostatic potential of the normal membrane is asymmetric, with a downhill slope in the potential on going from the outer leaflet to the inner leaflet [Fig.4]. This potential gradient could accelerate the diffusion of cisplatin from the outer to inner leaflets. In contrast, the electrostatic profile of the cancer membrane is

symmetric and rather flat, resulting in slow diffusion of cisplatin. In this context, we believe that changes in the electrostatic potential on going from normal to cancer membranes may change the interaction between cancer cells with surrounding, leading to changes in the elastic properties, whether softer or harder of cancer cells. However, this hypothesis needs to be studied further.

Concerning to the elastic moduli, the question is whether the calculated results depend on the employed method? As mentioned, the analysis of fluctuation of lipid orientation vector in Fourier space[31–33] method and the real space method[35] are currently widely used. It has been demonstrated that two methods yield to similar results with a difference up to 17% for different pure membrane models DPPC, DOPC and DOPE (see Supporting Information of Ref.[33]). Allolio et al. also calculated the elastic moduli of large variety of systems, including mixtures and curved membrane geometries, by using the real space and Fourier analysis methods. The authors found good agreement between the two methods.[36] Nevertheless, in addition to the results presented above obtained from the fluctuation analysis in the Fourier space, we also calculate the elastic bending modulus employing the real space method of Khelashvili et al.,[35] and as shown in Tab.3, the results of both methods are in good agreement. This indicates that our results are not biased due to the employed calculation methods, in agreement with the finding of Allolio et al.[36]

Due to the lack of experimental data, a direct comparison of our simulation results with experimental elastic moduli of multiple components lipid membranes is unfortunately impossible. Recently, Venable et al. carried out atomistic MD simulations for 12 fully hydrated single component bilayers.[34] Encouragingly, the values of the bending modulus K_c, calculated using Eq.1, were in near quantitative agreement with vesicle flicker experiments. Notably, an excellent agreement between simulation and experiment was obtained for DOPE membrane. This encouraging results give us a confidence that the elastic moduli of our membrane models would also be close to that of real membranes, although results are not directly compared to experiments. This suggests that the simulation approach could be

useful to study the mechanical property of cell membranes, and in particular, to compare the elastic property of the normal and cancer membrane models.

In this work, we focus on effects of the overexpression of the DOPS lipid in the outer leaflet and the reduction of cholesterol concentration on the elastic moduli of the cancer membranes. In our membrane models, the mole fraction of DOPS lipid was taken from the lipid contents of the mammalian erythrocyte membranes measured by experiments,[41–43] and the mole fraction of CHL is about the typical sterol concentration in the mammalian plasma membrane.[44] The simulation shows that (i) given the same cholesterol concentration, there are no clear evidences which show that the cancer membranes are softer than the normal counterparts. That is, the bending and tilt elastic moduli of the normal and cancer membranes are similar, and the twist modulus of a cancer membrane could be slightly softer than that of the normal counterpart or vice versa. This indicates that the overexpression of DOPS lipid in the outer leaflet may not be an essential factor that directly causes the softening of the cancer cells, but rather a biological cue related to the apoptotic pathway. As shown, however, the electrostatic potential of the membrane is altered due to the redistribution of PS lipids, and this could alter the interaction between cells with surrounding, thus resulting in indirectly changes in the elasticity of cancer cells. (ii) If the cholesterol concentration is reduced, then all elastic moduli of normal membranes are reduced, regardless of the overexpression in DOPS lipids in the outer leaflet (M1→M5*) or not (M1→M5). To explain this effect of cholesterol, we note that for a long time cholesterol is known to stiffen saturated lipid membranes, and recently, Chakraborty et al. have shown that cholesterol also increases the bending rigidity of unsaturated lipid membranes.[62–64] This suggests that cholesterol should also stiffen the membranes made up of a mixture of saturated and unsaturated lipids, which are the case of our membrane models. In this context, the reduction in cholesterol is one of the factors that causes the softening of cancer membranes. We should mention that the effect, which is caused by cholesterol on the structure of membranes, has been observed by experiments and simulations for various bilayer membrane systems.[13–17] However, we study, for the first

time, this effect on the elasticity property of normal and cancer membranes in this work. We note that the mole fraction of DOPS lipid in the outer leaflet is increased by $\sim$ 5-12% on transforming from the normal to cancer membranes [Tabs.1,2]. In a previous work, Doktorova et al. carried out MD simulations of a mixed POPC/POPS membrane containing 30% PS in each leaflet. The authors showed an opposite effect, that is the bending modulus of the POPC/POPS membrane is 22% larger than that of the pure POPC membrane.[37] This is consistent with theoretical consideration which predicts an increase in bending rigidity in the presence of charged lipids due to electrostatic repulsion between the lipid headgroups.[65,66] However, Jiang et al. recently carried out MD simulations of a pure POPC lipid membrane, and a mixed POPC/POPS membrane containing 20% POPS only in the inner leaflet. The simulations showed that the bending modulus of the POPC/POPS membrane is $\sim$ 20% smaller than that of the POPC membrane.[38] This finding was explained that the overall effect of POPS lipids on the bending modulus largely depends on the number of POPS lipid pairs as seen from Eq.4 . Thus, high mole fractions of PS are required to observe significantly effect on the bending modulus. In our membrane models, the mole fraction of the DOPS lipid is rather low, $\sim$ 5-12%, thus effect due to the overexpression of DOPS lipid in the outer leaflet on the elastic moduli is not evident.

The remaining question is whether our results can be related to experimental measurement of the softening of cells? Several experimental techniques, such as atomic force microscopy (AFM),[5] micropipette aspiration[4] and particle-tracking microrheology[3] have been developed to measure the stiffness of cells. However, results obtained from these method are usually inconsistent. This is probably due to the fact that each method measures different cell components. In AFM experiments, the applied force is the sum of forces from the cell membrane, cytoskeleton network, and cytosol. In the micropipette aspiration method the cell membrane and cytoskeleton influence the results, and in the particle-tracking microrheology method the contribution of cytoskeleton network is important. This fact indicates that all three components including the cell membrane, cytoskeleton network, and cytosol

contribute to the stiffness of cells. The cytoskeleton has long been considered to be the main factor affecting cell stiffness,[67] and this has motivated some researchers to try to adjust the cell stiffness by regulating actin microfilaments.[68] Very recently, Ren et al. have developed a physical model to analyze the AFM force relaxation curves, and shown that the softening of cancer cells is mostly due to the decreases of the membrane surface tension.[69] In a traditional AFM experiment, the membrane tension, σ, is estimated by measuring the force required to pull a membrane tether with radius of R_0 from bilayer membrane. It has been shown that σ is approximately related to the membrane bending modulus K_c as $\sigma = K_c/2R_0^2$.[70] This implies that, according to the study of Ren et al., the softening of cancer cells is mainly due to decreases of the membrane bending modulus. In this context, the reduction of the cholesterol concentration in the cancer membranes, which reduces the bending modulus K_c, may contribute, at least partly to the softening of the cancer cells, relative to the normal cells.

The present study has some limitations of which we are fully aware. First, for the lipid mixtures like our models, the coupling between compositions is a possible driving force for the formation of lipid rafts.[71] Although our simulation time is rather long (1 microsecond for each system), it seems unlikely that lipids are perfectly ideally mixed. This non-ideality could affect the local shape and density, which in turn affects the elasticity properties of the membrane. Nevertheless, as we already mentioned that our MD simulation and enhanced sampling simulation of Rivel et al.[24] give similar results on the structural properties of both normal and cancer models, we believe that effect due to limitation of sampling on the elasticity of membranes should be minor. Second, in reality, a cell membrane is populated with ensembles of membrane proteins, thus the effective elastic moduli of a membrane is contributed by both elastic properties of the lipid bilayer and of the proteins embedded within it.[72] Simulations of large complex lipid/proteins is infeasible at the moment, but will be pursued in future studies to study this hypothesis. Third, our membrane models have the same number of lipids in each leaflet, therefore, the area per lipid for the two leaflets

are kind of forced to be the same. In contrast, the biological membrane in reality can have different numbers of lipids in each leaflet, therefore, the area per lipid for the two leaflets can be different, thus the membrane can be curved, resulting in differences in the thickness and mechanical properties between the two leaflets. Indeed, Yesylevskyy et al. have recently carried out atomistic MD simulations to study the influence of the membrane curvature on the structural properties of the asymmetric membranes, and shown that the thickness, the order parameter of the lipid tails and A_L are different between the two leaflets.[73] Whether the elastic moduli of the two leaflets of the curved membranes are different requires further investigation.

Conclusion

We have carried out all-atom MD simulations of five normal membranes models and five cancer membrane models. The cancer membranes are constructed taking into account the overexpression of the DOPS lipids in the outer leaflet and the reduction of cholesterol concentration. Various structural quantities, including the area per lipid, membrane thickness, electron density, and order parameters of lipid tails are calculated for each membrane. Results show that at the same cholesterol concentration all these quantities are very similar between membranes, regardless of normal or cancer models. This indicates that the overexpression of the DOPS lipids in the outer leaflet does not affect significantly the structure of the normal or cancer membranes. The effect of cholesterol is more pronounced in both membrane types, showing that if the cholesterol concentration is reduced then the area per lipid becomes larger, membrane thickness is smaller and lipid chains are more disordered. We find that the electrostatic potential of the normal membrane is asymmetric with a downward slope when going from the outer to the inner leaflets. Meanwhile, the potential energy of the cancer membrane is symmetrical between the inner and outer leaflets. Therefore, the molecular transport across bilayer could be different between the normal and cancer mem-

branes, and this may cause indirectly differences in mechanical properties of two membrane types.

The elastic moduli of each membrane, including bending, tilt and twist constants are calculated using two different methods, and results of two methods are quite similar. At the same cholesterol concentration, the bending and tilt moduli of the normal and cancer membranes are very similar. However, the twist modulus of cancer membranes could be slightly larger or smaller than that of normal counterparts, depending on the models. Nevertheless, since only bending modulus contributes significantly to the stiffness of bilayers, thus our results imply that there is no clear evidence which indicates that the cancer membranes are softer than the normal counterparts. Thus, we conclude that the overexpression of the DOPS lipids in the outer leaflet also does not affect significantly the elasticity property of cancer membranes. However, it is of interest to see pronounced an effect, whether an increase or a decrease in the bending rigidity of our membrane models due to the overexpression of the DOPS lipids, by increasing the DOPS mole fractions in the models. This work is underway. Finally, we show that at low cholesterol concentrations, all three elastic moduli become smaller, implying that the reduction in cholesterol in cancer membranes could contribute partly to the softening of cancer cells.

Acknowledgments This work has been supported by the Department of Science and Technology at Ho Chi Minh City, Vietnam (grant 13/2020/HD-QPTKHCN), the "Initiative d'Excellence" program from the French State (Grant "DYNAMO", ANR- 11-LABX- 0011-01), the CNRS, the Narodowe Centrum Nauki, the National Science Foundation (NSF, grant SI2-SEE-1534941), the National Institute of Health (NIH K25AG070277) and the CINES/TGCC/IDRIS centers for providing computer facilities.

References

(1) Blackadar, C. B. Historical review of the causes of cancer. *J Clin Oncol.* **2016**, *7*, 54.

(2) Alibert, C.; Goud, B.; Manneville, J. B. Are cancer cells really softer than normal cells? *Biol. Cell* **2017**, *109*, 167.

(3) Wirtz, D. Particle-tracking microrheology of living cells: principles and applications. *Ann. Rev. Biophys.* **2009**, *38*, 301.

(4) Hochmuth, R. M. Micropipette aspiration of living cells. *J. Biomech.* **2000**, *33*, 15.

(5) Ding, Y.; Wang, J.; Xu, G.; Wang, G. F. Are elastic moduli of biological cells depth dependent or not? Another explanation using a contact mechanics model with surface tension. *SoftMatter* **2018**, *14*, 7534.

(6) Marquardt, D.; Geier, B.; Pabst, G. Assymmetric lipid membranes: towards more realistic model systems. *Membranes* **2015**, *5*, 180.

(7) Connor, J.; Bucana, C.; Fidler, I. J.; Schroit, A. J. Differentiation-dependent expression of phosphatidylserine in mammalian plasma membranes: quantitative assessment of outer-leaflet lipid by prothrombinase complex formation. *Proc. Natl. Acad. Sc. U.S.A* **1989**, *86*, 3184.

(8) Utsugi, T.; Schroit, A. J.; Connor, J.; Bucana, C. D.; Fidler, I. J. Elevated expression of phosphatidylserine in the outer membrane leaflet of human tumor cells and recognition by activated human blood monocytes. *Cancer Res* **1991**, *51*, 3062.

(9) Cruciani, R. A.; Barker, J. L.; Zasloff, M.; Chen, H. C.; Colamonici, O. Antibiotic magainins exert cytolytic activity against transformed cell lines through channel formation. *Proc. Natl. Acad. Sci. U. S. A.* **1991**, *88*, 3792.

(10) Wonderlin, W. F.; Woodfork, K. A.; Strobl, J. S. Changes in membrane potential during the progression of MCF-7 human mammary tumor cells through the cell cycle. *J. Cell. Physiol.* **1995**, *165*, 177.

(11) Gurtovenko, A. A.; Vattulainen, I. Membrane potential and electrostatics of phospholipid bilayers with asymmetric transmembrane distribution of anionic lipids. *J. Phys. Chem. B* **2008**, *112*, 4629.

(12) Simons, K.; Ikonen, E. How cells handle cholesterol. *Science* **2000**, *290*, 1721.

(13) Oldfield, E.; Meadows, M.; Rice, D.; Jacobs, R. Spectroscopic studies of specifically deuterium labeled membrane systems. Nuclear magnetic resonance investigation of the effects of cholesterol in model systems. *Biochemistry* **1978**, *17*, 2727.

(14) Urbina, J. A.; Pekerar, S.; Le, H.; Patterson, J.; Montez, B.; Oldfield, E. Molecular order and dynamics of phosphatidylcholine bilayer membranes in the presence of cholesterol, ergosterol and lanosterol: a comparative study using 2h-, 13C- and 31P-NMR spectroscopy. *Biochimica et Biophysica Acta - Biomembranes* **1995**, *1238*, 163.

(15) Thalia, T.; Mills, G.; Toombes, E.; Tristram-Nagle, S.; Smilgies, M.; Feigenson, G.; Nagle, J. F. Order parameters and areas in fluid-phase oriented lipid membranes using wide angle X-ray scattering. *Biophys. J* **2008**, *95*, 669.

(16) de Meyer, F.; Smit, B. Effect of cholesterol on the structure of a phospholipid bilayer. *Proc. Natl. Acad. Sci. USA* **2009**, *106*, 3654.

(17) Kucerka, N.; Tristram-Nagle, S.; Nagle, J. F. Closer Look at Structure of Fully Hydrated Fluid Phase DPPC Bilayers. *Biophys J.* **2006**, *90*, L83.

(18) Berger, O.; O.Edholm,; F.Jahnig, Molecular dynamics simulations of a fluid bilayer of dipalmitoylphosphatidylcholine at full hydration, constant pressure, and constant temperature. *Biophys. J* **1997**, *72*, 2002.

(19) D.P.Tieleman,; L.R.Forrest,; Sansom, M.; H.J.C.Berendsen, Lipid Properties and the Orientation of Aromatic Residues in OmpF, Influenza M2, and Alamethicin Systems: Molecular Dynamics Simulations. *Biochemistry* **1998**, *37*, 17554.

(20) Holtje, M.; Forster, T.; Brandt, B.; Engels, T.; von Rybinski, W.; Holtje, H. D. Molecular dynamics simulations of stratum corneum lipid models: fatty acids and cholesterol. *Biochim. Biophys. Acta* **2001**, *1511*, 156.

(21) Niemela, P.; Hyvonen, M. T.; Vattulainen, I. Structure and Dynamics of Sphingomyelin Bilayer: Insight Gained through Systematic Comparison to Phosphatidylcholine. *Biophys. J* **2004**, *87*, 2976.

(22) Bhide, S. Y.; Zhang, Z.; Berkowitz, M. L. Molecular dynamics simulations of SOPS and sphingomyelin bilayers containing cholesterol. *Biophys. J* **2007**, *92*, 1284.

(23) Polley, A.; Vemparala, S.; Rao, M. Atomistic simulations of a multicomponent asymmetric lipid bilayer. *J. Phys. Chem. B* **2012**, *116*, 13403.

(24) Rivel, T.; Ramseyer, C.; Yesylevskyy, S. The asymmetry of plasma membranes and their cholesterol content influence the uptake of cisplatin. *Sci. Rep.* **2019**, *9*, 5627.

(25) Klahn, M.; Zacharias, M. Transformations in plasma membranes of cancerous cells

and resulting consequences for cation insertion studied with molecular dynamics. *Phys. Chem. Chem. Phys.* **2013**, *15*, 14427.

(26) Ingolfsson, H. I.; Carpenter, T. S.; Bhatia, H.; Bremer, P.-T.; Marrink, S. J.; Lightstone, F. C. Computational Lipidomics of the Neuronal Plasma Membrane. *Biophys. J* **2017**, *113*, 2271.

(27) Helfrich, W. Elastic properties of lipid bilayers: theory and possible experiments. *Z. Naturforsch.* **1973**, *C28*, 693.

(28) Canham, P. B. The minimum energy of bending as a possible explanation of the biconcave shape of the human red blood cell. *J. Theor. Biol.* **1970**, *26*, 61.

(29) May, E. R.; Narang, A.; Kopelevich, D. I. Role of molecular tilt in thermal fluctations of lipid membranes. *Phys. Rev. E.* **2007**, *76*, 021913.

(30) Ryham, R. J.; Klotz, T. S.; Yao, L.; Cohen, F. S. Calculating Transition Energy Barriers and Characterizing Activation States for Steps of Fusion. *Biophys. J.* **2016**, *110*, 1110.

(31) Watson, M. C.; Penev, E. S.; Welch, P. M.; Brown, F. L. H. Thermal fluctuations in shape, thickness, and molecular orientation in lipid bilayer. *J. Chem. Phys.* **2011**, *135*, 244701.

(32) Watson, M. C.; Brandt, E. G.; Welch, P. M.; Brown, F. L. H. Determining biomembrane bending rigidities from simulations of modest size. *Phys. Rev. Letts* **2012**, *109*, 028102.

(33) Levine, Z. A.; Venable, R. M.; Watson, M. C.; Lerner, M. G.; Shea, J. E.; Pastor, R. W.; Brown, F. L. H. Determination of Biomembrane Bending Moduli in Fully Atomistic Simulations. *J. Am. Chem. Soc.* **2014**, *136*, 13582.

(34) Venable, R. M.; Brown, F. L. H.; Pastor, R. W. Mechanical properties of lipid bilayers from molecular dynamics simulation. *Chem. Phys. Lipids* **2015**, *192*, 60.

(35) Khelashvili, G.; Kollmitzer, B.; Heftberger, P.; Pabst, G.; Harries, D. Calculating the Bending Modulus for Multicomponent Lipid Membranes in Different Thermodynamic Phases. *J. Chem. Theory Comput.* **2013**, *9*, 3866.

(36) Allolio, C.; Haluts, A.; Harries, D. A local instantaneous surface method for extracting membrane elastic moduli from simulation: Comparison with other strategies. *Chem. Phys.* **2018**, *514*, 31.

(37) Doktorova, M.; Harries, D.; Khelashvili, G. Determination of bending rigidity and tilt modulus of lipid membranes from real-space fluctuation analysis of molecular dynamics simulations. *Phys. Chem. Chem. Phys.* **2017**, *19*, 16806.

(38) Jiang, W.; Lin, Y. C.; Luo, Y. L. Mechanical properties of anionic asymmetric bilayers from atomistic simulations. *J. Chem. Phys.* **2021**, *154*, 224701.

(39) Liu, Y. F.; Nagel, J. F. Diffuse scattering provides material parameters and electron density profiles of biomembranes. *Phys. Rev. E.* **2004**, *69*, 040901.

(40) Nagel, J. F. Introductory Lecture: Basic quantities in model biomembranes. *Faraday Discuss.* **2013**, *161*, 11.

(41) Daleke, D. L. Regulation of phospholipid asymmetry in the erythrocyte membrane. *Curr. Opin. Hematol.* **2008**, *15*, 191–195.

(42) abd R. F. A. Zwaal, A. J. V.; Roelofsen, B.; Comfurius, P.; Kastelijn, D.; van Deenen, L. The asymmetric distribution of phospholipids in the human red cell membrane. A combined study using phospholipases and freeze-etch electron microscopy. *Biochim. Biophys. Acta.* **1973**, *323*, 178.

(43) Zachowski, A. Phospholipids in animal eukaryotic membranes: transverse asymmetry and movement. *Biochem. J* **1993**, *294*, 1.

(44) van Meer, G.; Voelker, D. R.; Feigenson, G. W. Membran lipids: where they are and how they behave. *Nat. Rev. Mol. Cell. Biol.* **2008**, *9*, 112.

(45) Jr., A. D. M.; Bashford, D.; Bellott, M.; Dunbrack, R. L.; Evanseck, J. D.; Field, M. J.; Fischer, S.; Gao, J.; Guo, H.; Ha, S. et al. All-atom empirical potential for molecular modeling and dynamics studies of proteins. *J. Phys. Chem. B* **1998**, *102*, 3586–3616.

(46) Jorgensen, W. L.; Chandrasekhar, J.; Madura, J. D.; Impey, R. W.; Klein, M. L. Comparison of simple potential functions for simulating liquid water. *J. Chem. Phys.* **1983**, *779*, 926–935.

(47) Lindahl, E.; Hess, B.; van der Spoel, D. GROMACS 3.0: A Package for Molecular Simulation and Trajectory Analysis. *J. Mol. Mod.* **2001**, *7*, 306–317.

(48) Berendsen, H. J. C.; Postma, J. P. M.; van Gunsteren, W. F.; Dinola, A.; Haak, J. R. Molecular-Dynamics With Coupling to an External Bath. *J. Chem. Phys.* **1984**, *81*, 3684–3690.

(49) Darden, T.; York, D.; Pedersen, L. Particle Mesh Ewald: An N·log(N) Method for Ewald Sums in Large Systems. *J. Chem. Phys.* **1993**, *98*, 10089–10092.

(50) Gapsys, V.; de Groot, B. L.; Briones, R. Computational analysis of local membrane properties. *J Comput Aided Mol Des.* **2013**, *27*, 845.

(51) Allen, W.; Lemkul, J.; Bevan, D. GridMAT-MD: a grid-based membrane analysis tool for use with molecular dynamics. *J. Comput. Chem.* **2009**, *30*, 1952.

(52) Shahane, G.; Ding, W.; Palaiokostas, M.; Orsi, M. Physical properties of model biological lipid bilayers: insights from all-atom molecular dynamics simulations. *J. Mol. Model* **2019**, *25*, 76.

(53) Asawakarn, T.; Cladera, J.; O'Shea, P. Effects of the membrane dipole potential on the

interaction of saquinavir with phospholipid membranes and plasma membrane receptors of Caco-2 cells. *J. Bio. Chem.* **2001**, *276*, 38457.

(54) Vermeer, L. S.; de Groot, B. L.; Reat, V.; Milon, A.; Czaplicki, J. Acyl chain order parameter profiles in phospholipid bilayers: computation from molecular dynamics simulations and comparison with 2H NMR experiments. *Eur Biophys J* **2007**, *36*, 919–931.

(55) Sachs, J. N.; Crozier, P. S.; Woolf, T. B. Atomistic simulations of biologically realistic transmembrane potential gradients. *J. Chem. Phys.* **2004**, *121*, 10847.

(56) Heberle, F. A.; Feigenson, G. W. Phase Separation in Lipid Membranes. *Cold Spring Harb Perspect Biol* **2011**, *3*, a004630.

(57) Duwe, H. P.; Sackmann, E. Bending elasticity and thermal excitations of lipid bilayer vesicles: Modulation by solutes. *Phys. A* **1990**, *163*, 410.

(58) McMahon, H. T.; Boucrot, E. Membrane curvature at a glance. *J. Cell Sci.* **2015**, *128*, 1065.

(59) Shinoda, W. Permeability across lipid membranes. *Biochim Biophys Acta Biomembr.* **2016**, *1858*, 2254–2265.

(60) Chaudhary, J.; Munshi, M. Scanning electron microscopic analysis of breast aspirates. *Cytopathology* **1995**, *6*, 162.

(61) Dobrzynska, I.; Szachowicz-Petelska, B.; Sulkowski, S.; Figaszewski, Z. Changes in electric charge and phospholipids composition in human colorectal cancer cells. *Mol. Cell. Biochem.* **2005**, *276*, 113.

(62) Chakraborty, S.; Doktorova, M.; Molugu, T. R.; Heberle, F. A.; Scott, H. L.; Dzikovski, B.; Nagao, M.; Stingaciu, L. R.; Standaert, R. F.; Barrera, F. N. et al. How cholesterol stiffens unsaturated lipid membranes. *Proc. Natl. Acad. Sci. U. S. A.* **2021**, *117*, 21896.

(63) Nagle, J. F.; Evans, E. A.; Bassereau, P.; Baumgart, T.; Tristrm-Nagle, S.; Dimova, R. A needless but interesting controversy. *Proc. Natl. Acad. Sci. U. S. A.* **2021**, *118*, e2025011118.

(64) Ashkar, R.; Doktorova, M.; Heberle, F. A.; Scott, H. L.; Barrera, F. N.; Katsaras, J.; Khelashvili, G.; Brown, M. F. Reply to Nagle et al.: The universal stiffening effects of cholesterol on lipid membranes. *Proc. Natl. Acad. Sci. U. S. A.* **2021**, *118*, e2102845118.

(65) Winterhalter, M.; Helfrich, W. Bending Elasticity of Electrically Charged Bilayers - Coupled Monolayers, Neutral Surfaces, and Balancing Stresses. *Journal of Physical Chemistry* **1992**, *96*, 327.

(66) May, S. Curvature elasticity and thermodynamic stability of electrically charged membranes. *J. Chem. Phys.* **1996**, *105*, 8314.

(67) Calzado-Martin, A.; Encinar, M.; Tamayo, J.; Calleja, M.; Paulo, A. S. Effect of actin organization on the stiffness of living breast cancer cells revealed by peak-force modulation atomic force microscopy. *Acs Nano* **2016**, *10*, 3365.

(68) Gu, W. H.; Bai, X.; Ren, K. L.; Zhao, X. Y.; Xia, S. B.; Zhang, J. X.; et al., Monofullerenols modulating cell stiffness by perturbing actin bundling. *Nanoscale* **2018**, *10*, 1750.

(69) Ren, K.; Gao, J.; Han, D. AFM Force Relaxation Curve Reveals That the Decrease of Membrane Tension Is the Essential Reason for the Softening of Cancer Cells. *Front. Cell Dev. Biol.* **2021**, *9*, 663021.

(70) Ayee, M. A.; Levitan, I. Membrane Stiffening in Osmotic Swelling: Analysis of Membrane Tension and Elastic Modulus. *Curr Top Membr.* **2018**, *81*, 97.

(71) Giang, H.; Shlomovitz, R.; Schick, M. Microemulsions, modulated phases and macroscopic phase separation: a unified picture of rafts. *Essays Biocjem.* **2015**, *57*, 21.

(72) Netz, R. R.; Pincus, P. Inhomogeneous fluid membranes: Segregation, ordering, and effective rigidity. *Phys. Rev. E* **1995**, *52*, 4114.

(73) Yesylevskyy, S. O.; Rivel, T.; Ramseyer, C. The influence of curvature on the properties of the plasma membrane. Insights from atomistic molecular dynamics simulations. *Sci. Rep.* **2017**, *7*, 16078.